Pergamon

Continental Shelf Research, Vol. 15, No. 4/5, pp. 509–537, 1995

0278–4343/95 $9.50 + 0.00

0278–4343(94)00058–1

Acoustic scattering from zooplankton and micronekton in relation to a whale feeding site near Georges Bank and Cape Cod

MICHAEL C. MACAULAY,* KAREN F. WISHNER† and KENDRA L. DALY‡

(*Received* 7 *June* 1993; *in revised form* 1 *March* 1994; *accepted* 15 *May* 1994)

Abstract—This research was part of the South Channel Ocean Productivity Experiment (SCOPEX), a multidisciplinary study to investigate the biological and physical processes associated with the very high annual springtime abundance of right whales (*Eubalaena glacialis*) in the Great South Channel off New England. Right whales appear to gather there in the spring because of the increased abundance of aggregations of their principal prey, the copepod *Calanus finmarchicus*. Observations of hydroacoustic scattering were made in relation to the hydrography, whale distributions, and other biological measurements in the vicinity of the Great South Channel during May 1986, March, April and May of 1988, and May and June of 1989. Copepods were detected (at 200 kHz) as a near-surface layer with strong diel changes. In 1989, a second frequency (120 kHz) was used to discriminate between copepod layers (which the 120 kHz detected only weakly) and other targets (which both frequencies detected). Acoustically distinct layers of zooplankton and micronekton were observed, which were often correlated in time and space with the copepod layers. Quantitative estimates derived from the acoustic data indicate that the abundance of zooplankton varied from 1–5 g wet weight m^{-3} to 18–25 g wet weight m^{-3}, which correlates well with the abundances observed from MOCNESS tows. The acoustic data revealed a complex diel migration of two layers in addition to the copepods. Euphausiids (predominantly *Meganyctiphanes* sp.) were found in a layer above the bottom, and a mid-water layer may have been due to sand lance (*Ammodytes americanus*). The observed biological phenomena appeared to be related to the complex hydrography of the region. A surface thermal front existed at the northern entrance to the channel in 1988 and 1989, with colder vertically mixed water to the south and warmer stratified water to the north. A Fast Fourier Transform analysis for spectral composition and autocovariance shows (a) strong contrasts in the spectral density across one frontal feature (predominantly a salinity front) as opposed to away from the front, and (b) significant differences between those areas where a whale moved more rapidly (presumably searching for food) and where it spent more time (presumably or observably feeding). The behavior of whales, in particular the right whale, can be shown to be related to the spatial scales and abundance of their prey by the use of hydroacoustic estimates of target distribution and abundance.

INTRODUCTION

HYDROACOUSTIC observations were one component of a multidisciplinary study in the Great South Channel (GSC) between Georges Bank and Nantucket Shoals. Previous work by CETAP (1982) showed that during April and May large numbers of cetaceans (including right, fin, humpback, and minke wales, dolphins, and porpoises) aggregate in a

*Applied Physics Laboratory, University of Washington, Seattle, WA 98195, U.S.A.
†Graduate School of Oceanography, University of Rhode Island Narragansett, RI 02882, U.S.A.
‡Graduate Program in Ecology, University of Tennessee, Knoxville, TN 37923, U.S.A.

small region in the northern part of the GSC. Virtually the entire known northwest Atlantic population of the right whale (*Eubalaena glacialis*), an endangered species, may be found within the GSC at this time (KENNEY *et al.*, 1995). We hypothesized that this aggregation of right whales in the GSC during spring was due to an unusual abundance and/or degree of aggregation of their principal prey, the copepod *Calanus finmarchicus*.

The purpose of the SCOPEX project was to investigate the interactions between right whales and *C. finmarchicus* in the GSC area, and to determine the physical and biological processes responsible for the concentration of biological activity in this area. The observations presented here were collected on a pilot study from 19–22 May 1986 and on two longer cruises in 1988 (12–17 March, 26 April–16 May) and 1989 (8 May–12 June). The focus of our field effort was related to three main hypotheses: (1) distributions of acoustically censusable targets can be correlated with the hydrography and biology of the area; (2) concentration size, frequency of concentrations and identity of sound backscatterers in the part of the GSC where whales are abundant are different from those in nearby non-whale areas; and (3) whale behavior can be correlated with distribution of potential prey. We hoped to show that measured backscatter could be strongly correlated with the distribution and abundance of copepods, at least in the upper water column (less than 100 m).

MATERIALS AND METHODS

The hydroacoustic technique employed was echo-integration following the methods of THORNE (1971), CUSHING (1978), SWINGLER and HAMPTON (1981) and JOHANNESSON and MITSON (1983). The details of using echo-integration are well described in SWINGLER and HAMPTON (1981), the manual of methods by JOHANNESSON and MITSON (1983), and the book by MACLENNAN and SIMMONDS (1992). The amount of backscattered sound is related to the quantity or biomass of scattering organisms by applying a target strength for the type of target present. The units of target strength in this application are usually in logarithmic units of sound intensity (decibels, or dB) per unit weight of scattering organism, rather than per individual. If the ensonified aggregation is composed of a mixed population of targets, estimation of the biomass of targets is more difficult. However, the estimate of backscattered sound in unscaled (no target strength) logarithmic units (dB) is still a valid measure of general abundance.

The methodology of analyzing acoustic data by echo-integration is well established (MIDTTUN and NAKKEN, 1968; THORNE, 1971; MACAULAY, 1978; CUSHING, 1978; MATHISEN, 1980; JOHANNESSON and MITSON, 1983). The analysis of acoustic data from transects produced estimates of biomass along the cruise track by intervals of time (distance). In addition, vertical profiles of distribution and abundance were calculated for depth slices of selected thickness (usually 1–10 m). These vertical profiles were used for statistical comparison with hydrography and sampling by other components. This method of analyzing acoustic data has also been used to examine the distribution of krill (*Euphausia superba*) in the Antarctic (MACAULAY *et al.*, 1984; MATHISEN and MACAULAY, 1983). Statistical confidence limits were calculated in order to compare between and within areas, and false-color images were generated to illustrate the density structure of acoustically detected concentrations of zooplankton and micronekton.

Initial choice of frequency was made by using models of target strength and other acoustic parameters to select a frequency likely to produce measurable scattering from the

targets of interest. This process indicated that 200 kHz would detect concentrations of copepods and also be capable of censusing other targets at the depth ranges anticipated. This frequency had been used effectively to detect large copepods (BARRACLOUGH *et al.*, 1969) and *C. finmarchicus* in the Gulf of Maine (KOSLOW, personal communication). We used this frequency in all three studies and were able to detect layers of copepods and other targets as small as 1 mm where they were abundant (more than 100 individuals per m^3). In the third study (1989) we used an additional frequency of 120 kHz for comparison purposes.

The target strength to length relationships for copepods and other targets were based on measured values where possible or were computed using the model developed by KRISTENSEN (1983). This model is essentially the standard fluid-filled sphere model of JOHNSON (1977) and GREENLAW (1977) but with terms applied for resonance and orientation of the ensonified organism. Using measured values for sound speed and density contrast for copepods, the model estimated the target strength of a 1 mm (equivalent spherical diameter) individual to be −99 dB. This value was used to determine the target strength to weight relationship, −36 dB kg^{-1} of copepods (assuming an average wet weight of approximately 0.24 mg per 1 mm individual). The −36 dB kg^{-1} value was used in the integration of the 200 kHz data. Such sphere models undoubtedly oversimplify the sound scattering, and hence the estimated target strength, even from small targets; however the estimated target strength for an individual agrees well with recent, direct measurements of copepod target strength (RICHTER, 1985; WIEBE *et al.*, 1990). Other acoustic targets were identified as *Meganyctiphanes* sp. These auphausiids were predominantly 25–30 mm in length and would have a target strength of −75 dB. Assuming an average wet weight of 200 mg per individual would give −38 dB kg^{-1}. While every attempt was made to separate identifiable concentrations of non-copepod targets from the acoustic data, it was clear from the net catch data that some of the observed intensity of sound scatter was attributable to euphausiids in the upper 50 m. The estimated biomass values as reported in this paper were computed using a single target strength of −36 dB kg^{-1}. The efficiency of capturing large euphausiids with the MOCNESS net at the speeds employed (less than 2 knots) was considered inadequate to sample them very quantitatively, making apportionment of biomass, in some depth ranges, indeterminate as to causative organism. The net effect of using the −36 dB target strength for all such cases will be an underestimate of actual total biomass (e.g. −36 dB of scatter would be reported as 1 kg, whereas using −38 dB would indicate there was 1.6 kg of biomass, an underestimate of 0.6 kg).

Because some of the estimated biomass data undoubtedly contain scattering from euphausiids, target-strength-free values are provided (in figure captions) for comparison with other acoustic studies. One commonly used scale for expressing acoustic scattering, in target-strength-free form, is volume backscattering strength (S_v), which has the units of dB and expresses the intensity of sound from a unit volume (1 m^3 at 1 m from the transducer). Two scales used for integrated sound intensity are column scattering strength (CSS) in units of dB m^{-2} and mean volume backscattering strength (MVBS) in units of dB.m^{-3}. The former (CSS) is total backscatter for a column of specified depth range, while the latter represents the mean backscattering value for a specific depth range. CSS values have stated or implied depth intervals as inherent parts of their calculation, making comparisons difficult where depth intervals are not the same. MVBS values can be used to compare acoustic estimates from study-to-study where specified integration intervals are only

Table 1. *Sounder system constants for acoustic systems used in* 1988 (200 kHz *only*) *and* 1989 (*both frequencies*)

	Constant (1988)	Constant (1989)
Manufacture/model	BIOSONICS INC. Model 101	BIOSONICS INC. Model 101
Frequency	120.0 kHz	200.0 kHz
Source Level	217.0 dB//1 μPa ref 1 m	216.4 dB//1 μPa ref 1 m
Receive Sensitivity	−126.5 dB//1V per μPa	−128.0 dB//1V per μPa
Pulse Length	435.0 μsec	435.0 μsec
Beam Pattern Direct.	−26.51 dB	−29.49 dB
TVG	digital	digital

approximately the same. A cautionary note in such comparisons is that because the MVBS was calculated for a specific interval, some targets and their contribution to the backscattering level may have been eliminated (i.e. outside of the interval). This note is particularly important where evidence exists for diel migration by particular targets. In this paper, all MVBS values were computed for 1 m depth bins, and are numerically equivalent to S_v.

The number of acoustic frequencies used and dates of the three surveys were different. In May 1986, the GSC area was surveyed using a single frequency (200 kHz) in a downward-directed mode. The transducer was towed from the starboard side of the R.V. *Delaware II* and was slightly behind the bow wake at a depth of 1–1.5 m. The 1988 GSC survey on the R.V. *Endeavor* was in two parts, the first 12–17 March and the second 26 April–16 May. A single frequency (200 kHz) system was deployed for both surveys, again towed at a depth of 1–1.5 m. The 1989 GSC survey (8 May–12 June) used two frequencies (120 kHz and 200 kHz) to examine some of the size—specific scattering, especially from copepods, as distinct from other zooplankton and fish. As in 1986 and 1988, acoustic observations were collected with a fin depth of 1–1.5 m.

All integration data were recorded in digital format for rapid data processing. Some information was displayed in real time as paper chart records and oscilloscope traces for use in directed sampling by nets and pumps. After the field sampling, the electronic and acoustic systems were calibrated at the Applied Physics Laboratory (APL) of the University of Washinton. APL calibration methods followed those set by the AMERICAN NATIONAL STANDARDS INSTITUTE (1972) and used a hydrophone calibrated at the Naval Research Laboratory, Orlando, Florida. Beam pattern, source level, and receive sensitivity were measured to within 1 dB (Table 1). Frequent (every 3 h) internal checks of system operation were done in the field using stable calibrators. The 120-kHz system used a transducer with a slightly wider beam pattern than the 200-kHz system, but otherwise the operating characteristics were similar (see Table 1).

A number of statistical methods were used to establish relationships of acoustic data (as an estimator of copepod abundance) to other biological sampling and to the hydrography. These included: cluster analysis and stepwise discriminant function analysis to develop indicators for whale vs non-whale areas, and spectral analysis using an FFT (Fast Fourier Transform) to compare the spatial scales of patch structure between areas. All the data used in the FFT were first detrended by using a linear model and filtered using a Hamming or Tukey window (HAMMING, 1977); then selected segments were examined for spectral

density and autocorrelation. These analyses were done using BMDP (1990) package of statistical programs.

The accoustic and environmental properties characterizing whale and non-whale sites and whale-feeding vs non-feeding locations were defined using data from a variety of sources. Acoustic data included the distribution of identified and unidentified targets and surface and subsurface hydroacoustic estimates of sound scatterers. Zooplankton biomasses and abundances from vertically stratified 1 m^2 MOCNESS plankton net tows (335-μm mesh nets), taken near or simultaneously with the acoustic measurements, were used to directly identify targets and for quantitative comparison. The processing and analyses of the MOCNESS catches are described by WISHNER *et al.* (1995). Briefly, the tows used here were vertically stratified with depth intervals for each net of: near-bottom to 90 m, 90–50 m, and 50–25 m, with the remaining five nets in 5 m intervals up to the surface. The peak copepod biomass is the total wet weight biomass of all copepods (mg m^{-3}) in the one net having the highest copepod biomass within a tow. Peak copepod biomass includes only the copepod-sized fraction, primarily *C. finmarchicus*. The depth range of the net with the peak abundance varied between years and locations and with the cycle of diel migration. Total water-column wet-weight biomass (mg m^{-2}) from the MOCNESS tows was also used in some analyses. Hydrographic data (surface and subsurface temperature and salinity) were obtained from CTD casts either as part of the regional surveys or in conjunction with net tows. Hydrographic sampling and results are described in LIMEBURNER and BEARDSLEY (1989) and CHEN *et al.* (1995a,b). For comparing whale and non-whale areas, a whale site was considered to be a location where right whales had been observed within the vicinity of the ship within 24 h. Observations of whale distribution and feeding behavior were made by trained observers (WINN *et al.*, 1995; KENNEY *et al.*, 1995).

The cluster analysis used single linkage method on standardized data (z-transform) which initially included hydrographic observations. The z-transform (or percentage transform) was used to remove the effect of the different numeric scales for the parameters selected. The data from 1988 and 1989 were examined to find pairs of day and night observations at the same or nearly the same locations (Table 2). These data were then classified into observations at locations with right whales and those without whales (W and N respectively in the column labeled WNW). Observations from 1988 are denoted in the ID column by M7 and those from 1989 are indicated by M9; the remaining characters are the MOCNESS net number. Because of the differences between day and night sound scatter, all observations (net and acoustic) were selected from the available measurements into pairs of day–night observations from the same locality. This greatly reduced the number of observations available for cluster and other analyses, but resulted in a data set which should minimize the effect of day–night differences. The intent was to objectively compare whale–non-whale sites, in a pair-wise manner, and thus reveal any predictive patterns to these two categories which might be present.

Those items found to be significant in clustering the data into whale and non-whale groupings were used to construct a discriminant function for testing data from other sites. The available data were divided into a set of observations that were used to develop the discriminant function and a subset ("Test" data in Table 2 and Table 3), which were reserved to test the discriminant function. The stepwise discriminant analysis program used (BMDP-7M) allows for testing the rigor of a discriminant function developed on one set of data against such a reserved data set, where the classification of the reserved set of

Table 2. Net catch and acoustic data used in cluster analysis and discriminant function analysis

Classified

Case	ID	GMT	WNW	DN	Dive	CPK	CPZ	EUP	EUZ	CP50	EU50	AZ	ACOUS
1	M706	123.05	N	N	d	3523	5	34	51	3253	34	11	2100
2	M707	123.15	N	D	d	1062	28	5	25	1062	5	12	970
3	M713	125.17	N	N	d	2116	2	66	90	2116	0	14	1740
4	M714	126.05	N	D	d	2339	3	1188	19	2339	1188	13	2400
5	M715	127.17	W	N	D	2472	83	47	24	80	47	8	24,020
6	M717	128.02	W	D	D	4501	24	0	90	4501	0	15	25,120
7	M902	141.06	N	N	s	1656	46	273	46	1656	273	45	3200
8	M903	141.12	N	D	s	823	146	13	146	535	4	10	1800
9	M912	144.03	W	N	S	12,795	20	636	8	12,795	636	32	12,800
10	M915	144.15	W	D	S	499	20	40	151	499	0	11	2560
11	N927	148.02	N	N	s	3974	2	901	24	3974	901	11	3200
12	M932	148.19	N	D	s	4531	13	142	246	4531	0	9	1600
13	M935	150.02	W	N	S	8359	14	7112	4	8359	7112	13	13,600
14	M934	149.19	W	D	S	6906	14	60	14	6906	60	19	34,400

Test

Case	ID	GMT	WNW	DN	Dive	CPK	CPZ	EUP	EUZ	CP50	EU50	AZ	ACOUS
15	M708	124.13	W	D	D	1241	53	67	92	1241	0	14	24,180
16	M711	125.01	W	N	D	4284	11	2567	11	4284	2567	11	22,490
17	M905	142.06	N	N	s	1311	28	68	50	1311	68	22	3360
18	M906	142.14	N	D	s	3926	14	25	157	3926	12	13	560
19	M919	145.03	W	N	S	2417	15	4284	4	2417	4284	22	26,480
20	M922	146.14	W	D	S	6237	8	84	87	6237	0	8	24,000
21	M937	150.08	W	D	S	6263	2	29	2	6263	29	10	11,470
22	SEGA	157.05	W	N	s	*	*	*	*	*	*	25	16,000
23	SEGB	157.05	W	N	s	*	*	*	*	*	*	25	25,140
24	SEGC	157.10	W	D	s	*	*	*	*	*	*	25	15,500

Case = case number; ID = M for MOCNESS tow (M7 = 1988, M9 = 1989), SEG for segment; GMT for day and nearest hour; WNW = whale area W or non-whale area N; DN = day–night; Dive = whale dive profile deep or shallow, with roman capital letter denoting observations used for 1988–1989 comparison; CPK = copepod peak biomass from the MOCNESS (mg m^{-3}); CPZ depth of the copepod peak biomass (m); EUP = euphausiid peak abundance from the MOCNESS (number 1000 m^{-3}); EUZ = depth of the euphausiid peak abundance (m); CP50 = copepod peak in upper 50 m from the MOCNESS (mg m^{-3}); EU50 = euphausiid peak in upper 50 m (number 1000 m^{-3}); AZ = depth of acoustic biomass peak (m); ACOUS = acoustic biomass at peak depth from the acoustic system (mg m^{-3}). All depths for MOCNESS samples are given as the midpoint of the net tow.

observations is known. Originally the data set also included hydrographic parameters, but these were not found to be significant in terms of determining clusters and are not included here. The spatial scale of patchiness in relation to frontal features and whale areas was determined by spectral analysis for a small-scale survey and a whale-tracking survey in which we followed the progress of a radio-tagged whale as it foraged for food. The observations labeled SEGA-SEGC were peak acoustic biomass estimated for copepods taken from specific sections of the whale-tracking survey. The data used in the spectral analysis were estimates of abundance at 100-m intervals along the trackline. Means, standard deviations, and coefficients of variation for all observations are provided (Table 3).

Table 3. Means, standard deviations and coefficients of variation for the data used in the stepwise discriminant analysis. Whale areas were defined as right whale sightings in the last 24 h; non-whale areas were those where either no whales were sighted or the presence of whales was unknown. Test data were from additional net and acoustic observations known to be from either whale or non-whale areas. These additional samples were used as a test data set for the discriminant function analysis

Means	Classified		Test	
Variable	Non-whale	Whale	Non-whale	Whale
CPK	2469.25	5922.00	2618.50	4792.13
EUP	340.75	1315.83	46.50	1372.00
CP50	2433.25	5323.33	2618.50	4792.13
EU50	300.62	1309.17	40.00	860.00
ACOUS	2.12	18.75	1.96	20.86

Standard deviations

	Classified		Test	
Variable	Non-whale	Whale	Non-whale	Whale
CPK	1342.86	4415.34	1849.08	1959.88
EUP	452.77	2849.70	30.40	1467.90
CP50	1396.11	4873.37	1849.08	1959.88
EU50	474.47	2853.33	39.60	1487.31
ACOUS	0.77	11.29	1.98	5.52

Coefficients of variation

	Classified		Test	
Variable	Non-whale	Whale	Non-whale	Whale
CPK	0.544	0.746	0.706	0.408
EUP	1.329	2.166	0.654	1.070
CP50	0.574	0.882	0.706	0.408
EU50	1.578	2.179	0.990	1.101
ACOUS	0.366	0.602	1.010	0.267
Number	8	6	2	8

RESULTS

In 1986, the GSC area was surveyed (Fig. 1) with a short break at some stations to take a bongo net haul, a neuston net tow, and an XBT cast. Some stations consisted of only an XBT cast so that the acoustic sampling was not interrupted. The survey track was planned to intersect at nearly right angles with a dominant hydrographic feature, a temperature front, which closely paralleled the 100-m isobath (Fig. 1).

A strong scattering layer near the surface was found to be copepods (predominantly *C. finmarchicus*). The deep scattering layer was predominantly euphausiids (*Meganyctiphanes* sp.). Additional targets that had a patchy distribution were also seen in mid-water (50–75 m) and often extending to the surface. This layer may have been sand lance

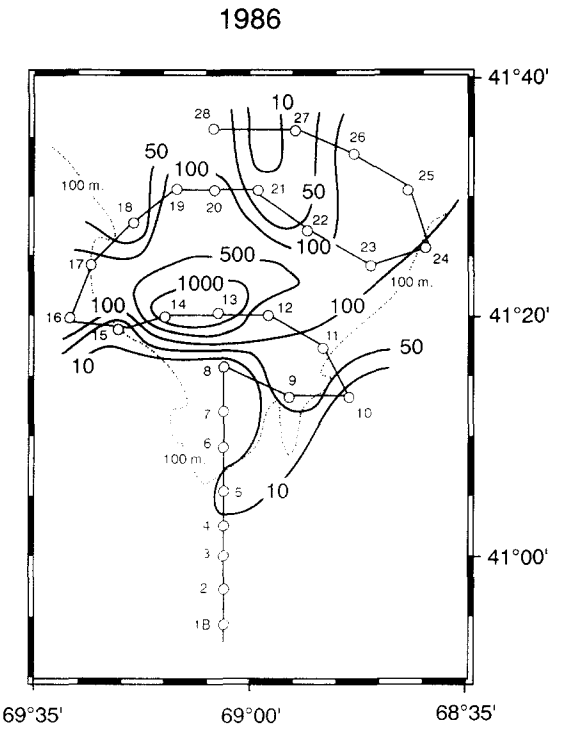

Fig. 1. Contour plot of data from 1986 pilot study. Integration interval was 3–73 m. Densities are shown in g m^{-2} for this interval. Conversions to target strength free CSS and MVBS for the indicated values are (respectively): 10 = −56 dB m^{-2}, −75 dB m^{-3}; 50 = −49 dB m^{-2}, −68 dB m^{-3}; 100 = −46 dB m^{-2}, −65 dB m^{-3}; 500 = −39 dB m^{-2}, −58 dB m^{-3}; 1000 = −36 dB m^{-2}, −55 dB m^{-3}. The cruise track is indicated by the solid line with open circles; the dashed line indicates the position of the 100-m isobath.

(*Ammodytes americanus*) though the sampling of this layer by bongo net and MOCNESS yielded few specimens, probably due to low net speeds of 1–1.5 knots. The euphausiid layer was strongly influenced by water-column depth and the presence of the scattering layer containing euphausiids ceased when the water depth was shallower than 50 m. The peak acoustic abundance was greater than 500 g m^{-2} (using −36 dB target strength).

The study area was characterized by a strong diel change in acoustic scattering layers at dawn and dusk. There was a pronounced vertical spreading out of the mid-water and deep scattering layers after 2000 (local time) and a matching concentration and sinking of layers after 0400 (local time). The surface copepod layer, however, only showed a slight vertical thickening at night and thinning during the day. Observations of actively feeding whales were very strongly associated with the surface copepod layers especially when a strong mid-water layer was present as well. These results and other biological data are discussed further in WISHNER *et al.* (1988).

A contour plot with overlain cruise track for the 1988 surveys is shown in Fig. 2. Acoustic observations were recorded continuously along all transect lines and sometimes between transects, as time permitted. In March, hydroacoustic observations were made in conjunction with eight MOCNESS tows (Fig. 2, upper panel). Results indicated a diffuse

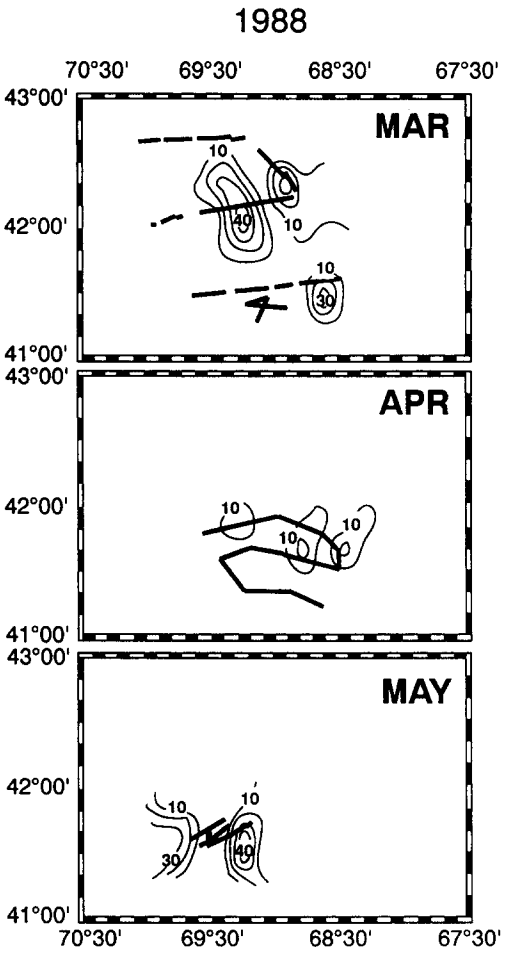

Fig. 2. Contour plots of data from March, April and May 1988 surveys. Integration interval was 3–50 m. Densities are shown in g m^{-2} for this interval. Conversions to target strength free CSS and MVBS for the indicated values are (respectively): 10 = −56 dB m^{-2}, −73 dB m^{-3}; 40 = −50 dB m^{-2}, −67 dB m^{-3}. The thick lines indicate the cruise track; broken segments indicate interruptions for net tows and other operations. The data shown in each panel are from the month indicated in the upper right corner of each panel.

concentration of acoustic targets. However, some mid-water patches similar to those found in 1986 (thought to be sand lance) also were found in 1988. Occasional near-surface patches of copepods (again predominantly *C. finmarchicus*) and layers of euphausiids (*Meganyctiphanes* sp.) were observed. During the second leg in April–May, observations were made along some portions of transects and in conjunction with 23 MOCNESS tows and a number of bongo tows (Fig. 2, middle panel). Mid-way in the cruise, a small survey was completed in the vicinity of feeding whales (Fig. 2, lower panel). Unfortunately, the acoustic fin broke from the towing cable and was lost on 7 May.

The pattern of acoustic targets was strongly developed by May of 1988. Zooplankton and fish were abundant targets; acoustic concentrations were similar to those observed in May 1986, but median and maximum net tow abundances were lower. Frequent patches of

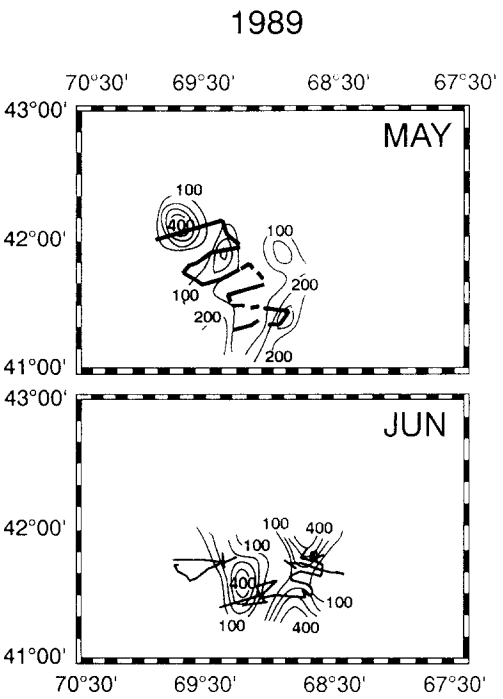

Fig. 3. Contour plots of data from May and June 1989 surveys. Integration interval was 3–50 m. Densities are shown in g m^{-2} for this interval. Conversions to target strength free CSS and MVBS for the indicated values are (respectively): 100 = −46 dB m^{-2}, −63 dB m^{-3}; 200 = −43 dB m^{-2}, −60 dB m^{-3}; 400 = −40 dB m^{-2}, −57 dB m^{-3}. The thick lines indicate the cruise track; broken segments indicate interruptions for net tows and other operations. The data shown in each panel are from the month indicated in the upper right corner of each panel.

copepods were found near-surface in some locations. Euphausiid layers were well defined and there were more fish schools (assumed to be sand lance) than the March 1988 leg. Many large fish targets were observed near bottom, and a strong diel shift in distribution was apparent.

Overall the scattering intensity was much less than in 1986; the peak acoustic abundance was less than 100 g m^{-2} in 1988 (using −36 dB target strength). These peak values were found at a limited number of locations within the 40 g m^{-2} contours in both March and May (i.e. too small to be shown on the scale of Fig. 2).

During the 1989 survey (Fig. 3), occasional near-surface patches of copepods (*C. finmarchicus*) and layers of euphausiids (*Meganyctiphanes* sp.) were observed, with a strong contrast between 120 kHz and 200 kHz signals for copepod layers but not for fish and euphausiid layers. Overall the scattering intensity was less than in 1986 but more than in 1988. The peak acoustic abundance was less than 500 g m^{-2} in 1989. During the May–June cruise, observations were made along some portions of transects and in conjunction with 46 MOCNESS tows and a number of bongo tows (Fig. 3, upper panel), as well as some special surveys in the vicinity of surface slicks and thermal fronts, and during a brief whale tracking survey (Fig. 3, lower panel). The acoustic data again showed a pattern in the kinds of scattering associated with the proximity to feeding whales, first observed in 1986. These consist of the presence of mid-water aggregations of (presumably) sand lance,

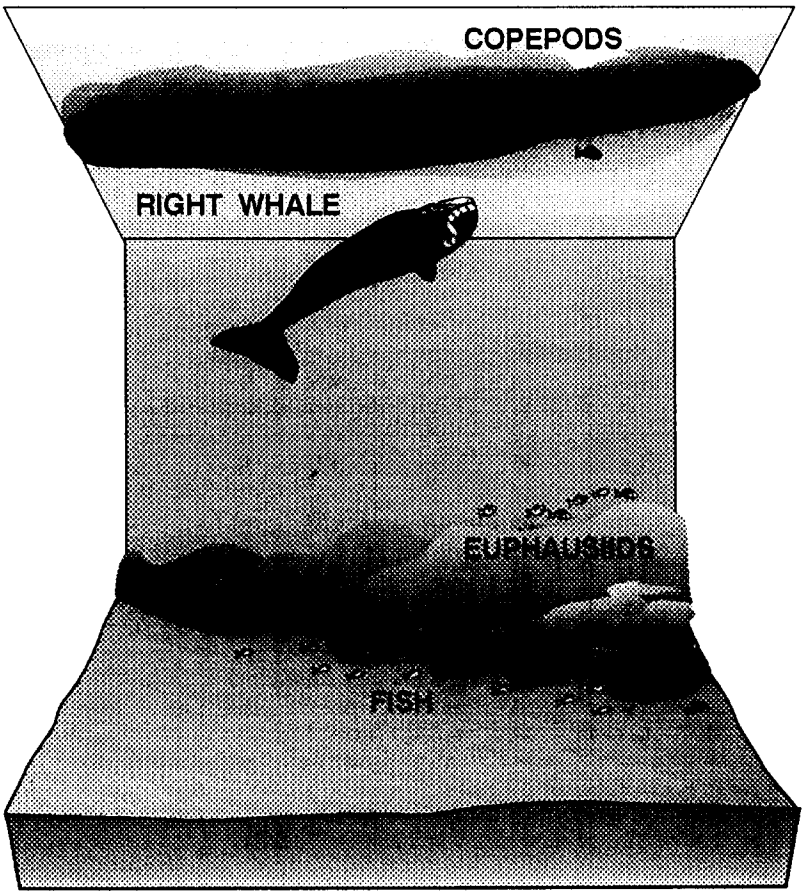

Fig. 4. Schematic diagram of a whale feeding area showing the major features present in most such sites.

surface concentrations of copepods, and deeper layers of euphausiids. This pattern associated with whale sites is schematically shown in Fig. 4.

The peak copepod water-column biomass from the MOCNESS tows was 181 g m^{-2} in 1986, 241 g m^{-2} in 1988, and 550 g m^{-2} in 1989. This is in comparison with acoustic estimates of over 500 g m^{-2} in 1986, less than 100 g m^{-2} in 1988, and somewhat less than 500 g m^{-2} in 1989. Some of these differences were due to the way the net sampled the water column (often not sampling the most dense concentrations of copepods, because of their patchy distribution) compared to the continuous nature of the acoustic sampling. The lower acoustic estimates for 1988 and 1989 are likely due to underestimation by the hydroacoustic system for copepods deeper than 75 m (due to the diminished sensitivity to concentrations of copepods at depths greater than 75 m and especially for targets with the size of the copepod lifestages present). The net estimates include sampling depths greater than 75 m, and the acoustic system often sampled depth intervals the net did not sample, because the net was towed obliquely through the water column, while the acoustic depth intervals were vertical. Table 4 shows a comparison of the biomasses of total zooplankton

Table 4. Comparison of MOCNESS samples and acoustic estimates for the same depth intervals

Case	ID	GMT	WNW	DN	MBT	MBC	A/CP50	A/MBT
1	M706	123.02	N	N	549	545	0.65	3.83
2	M707	123.15	N	D	563	563	0.91	1.72
3	M713	125.17	N	N	198	–	0.82	8.79
4	M714	126.05	N	D	676	574	1.03	3.55
5	M715	127.17	W	N	15	12	300	1600
6	M717	128.02	W	D	4270	4189	5.58	5.88
7	M902	141.06	N	N	1728	1656	1.93	1.85
8	M903	141.12	N	D	535	535	3.36	3.36
9	M912	144.03	W	N	11,214	11,104	1.00	1.14
10	M915	144.15	W	D	146	146	5.13	17.5
11	M927	148.02	N	N	3694	3644	0.81	0.87
12	M932	148.19	N	D	4531	4531	0.35	0.35
13	M935	150.02	W	N	8508	8359	1.63	1.60
14	M934	149.19	W	D	1823	1823	4.98	19.00
15	M708	124.13	W	D	67	–	19.5	361
16	M711	125.01	W	N	4904	4176	5.25	4.59
17	M905	142.06	N	N	1349	1311	2.56	2.49
18	M906	142.14	N	D	3926	3926	0.14	0.14
19	M919	145.03	W	N	1406	1312	11.0	18.8
20	M922	146.14	W	D	6237	6237	3.85	3.85

Case = case number; ID = M for MOCNESS tow (M7 = 1988, M9 = 1989), SEG for segment; GMT for day and nearest hour; WNW = whale area W or non-whale area N; DN = day–night; MBT = MOCNESS total biomass (mg m^{-3}) at depth that spanned the depth AZ (given in Table 2) for the particular sample; MBC = MOCNESS copepod biomass (mg m^{-3}) at depth that spanned the depth AZ (given in Table 2); A/CP50 = acoustic peak biomass (from Table 2) divided by copepod peak biomass in upper 50 m (from Table 2); A/MBT = acoustic peak biomass (from Table 2) divided by MOCNESS total biomass (from column labeled MBT).

and the copepod-sized fraction from the MOCNESS nets for the same tows and depth intervals as the peak biomasses shown in Table 2. In 17 of the 20 cases, the acoustic estimates of peak copepod biomass are larger than the net sample estimates. In seven of the 17 cases, the peak abundances from the acoustic data are within a factor of 2 of the net estimate for the upper 50 m (see Table 4, column labeled A/CP50). This factor was computed from the peak acoustic estimate in the upper 50 m (taken from Table 2) divided by the peak MOCNESS biomass for the upper 50 m (taken from Table 2). In ten of the 17 comparisons, the two estimates are within a factor of 4 of each other.

An examination of the ability of the two frequencies of hydroacoustic observation (120 kHz and 200 kHz) to separate targets by size is shown in Fig. 5. This figure contrasts hydroacoustic estimates of target abundance for two sites in the small-scale survey area with matched pairs of lower frequency (120 kHz), predominantly non-copepod targets, and higher frequency (200 kHz), copepod plus other target data. The displayed data are in units of dB m^{-3}. The identities of target organisms were determined from stratified MOCNESS samples from the component layers. In most cases, sound scatter from copepods was at or just below the threshold of detection used for the 120 kHz system, except where very dense concentrations of copepods were present (Fig. 5, lower). Selective thresholding of the 120 kHz data, to further reduce its ability to detect copepods, allowed comparisons of the data at the two frequencies to be used to suggest target identity

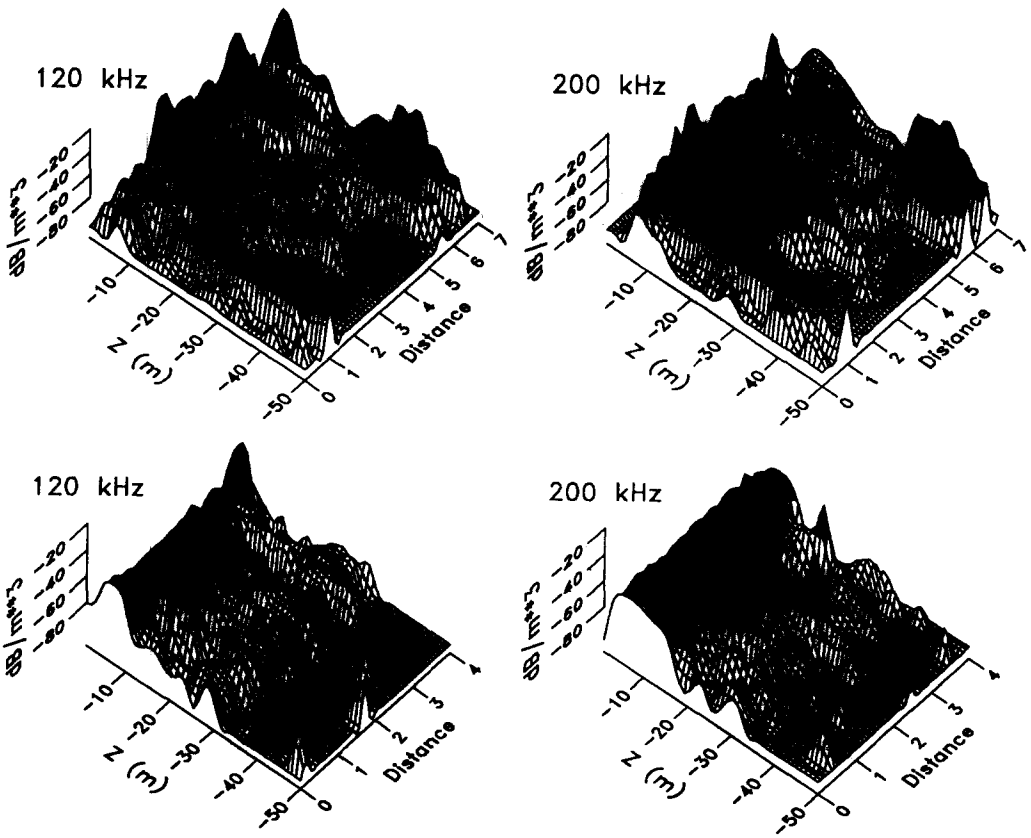

Fig. 5. Upper, 120 kHz vs 200 kHz comparison of vertical distributions in an area of low-moderate copepod abundance. Lower, 120 kHz vs 200 kHz comparisons of vertical distributions in an area of moderate-high copepod abundance. The data are presented as surface plots of mean volume scattering strength (MVBS, in dB m^{-3}). Note the lower intensity of surface copepod scattering in the 120 kHz plot is shown by the lesser amount of dark shaded area, representing those parts of the plot greater than −80 dB used as a thresholding value. The minimum level, which was used as a noise limit, is −95 dB m^{-3}.

(e.g. copepod layers) where no net samples were available to confirm that identity. Initially, threshold values were determined where samples were available and then those threshold values were used in areas where only acoustic data were available. The threshold level was −80 dB which was at least 15 dB above the minimum signal level considered to exceed the noise floor at −95 to −98 dB.

The distribution of acoustically detected biomass in the interval from 3 m to the bottom for a small-scale study conducted on 2–3 June 1989 in the vicinity of a salinity front (Fig. 6) showed a strong contrast in distribution across the frontal boundary. The front extended across the area shown at approximately 41.41°N and was associated with the presence of surface slicks and other visible changes in the appearance of the sea surface. The contouring shown in Fig. 6 produced some features which were unconfirmed by direct observation particularly for areas distant from the cruise track. Such features may be ignored, though the contouring method (kriging) has proven effective at accurately

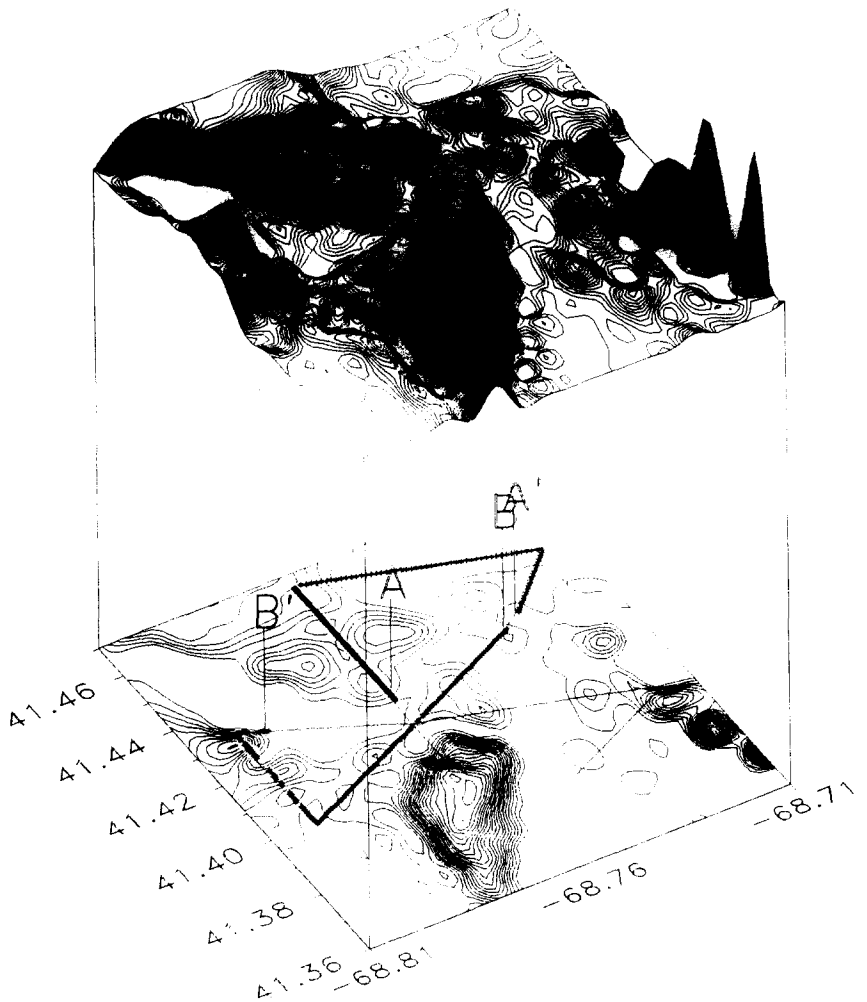

Fig. 6. Contour plot of 2 June 1989 survey with an overlay of spectral density segments and cruise track. The line segments shown in the lower plot (A–A', B–B') correspond to the segments of data that were used for analysis of spectral density. Peak abundance for each segment is given in Table 2 and the plot of spectral density is Fig. 8. Some features (especially those distant from the cruise track) are extrapolations from trends in the data (see the peaks in the corner near 68.71 W).

predicting the location of zooplankton concentrations in other studies (MACAULAY and MATHISEN, 1991; LOEB *et al.*, 1993). The backscattering intensity (as CSS and MVBS) for these two segments (Fig. 7) showed that the levels of backscatter encountered north of the front (segment A–A') were lower than those encountered south of the front (segment B–B') and that segment B–B' had a slightly greater frequency of peak abundances. The spectral density and autocovariance for these data (Fig. 8) were strongly contrasting. Major differences in patch size (indicated by the cycles km^{-1}) occurred in the range of 2–4 cycles km^{-1}, corresponding to an aggregation size of 0.5–0.25 km (i.e. the reciprocal of the frequency). The spectral density plot for segment A–A' contains component frequencies which are greater in magnitude at large-scales (less than 1 cycle km^{-1}) with progressively

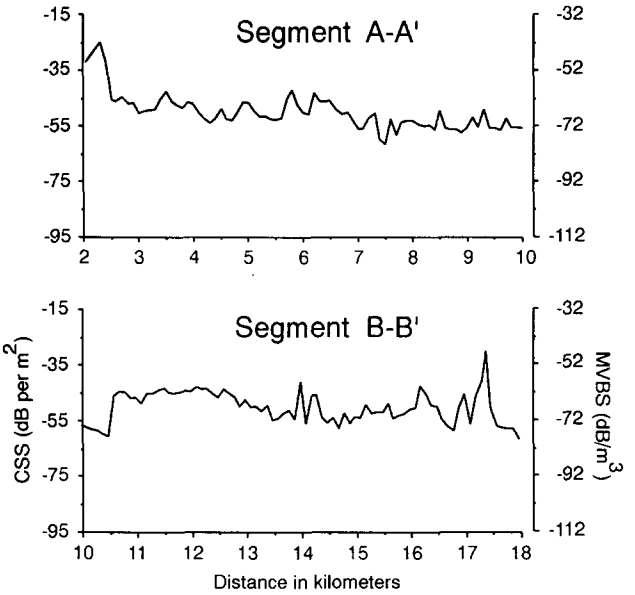

Fig. 7. Target strength free backscatter as column scattering strength (CSS) and mean volume backscattering strength (MVBS) for the line segments shown in Fig. 6. Distance from the start of the survey is given in km.

fewer component frequencies at small scales until 4 cycles per kilometer when there is a slight increase. The spectral density plot for segment B–B′ shows a flat spectrum containing component frequencies with nearly equal magnitude for all scales of distributions south of the front. Figure 9 shows a schematic representation of some of these acoustic biomass features (including surface manifestations) and represents a section taken N–S across the front, approximately in the middle in Fig. 6.

During 6 June 1989 we surveyed the distribution of copepods in the vicinity of a radio-tagged right whale. We followed behind it observing its behavior in response to the distribution of copepods (Fig. 10). At this locality there were few indications of zooplankton other than copepods (as indicated from comparisons of the 120-kHz and 200-kHz data) and no indications of fish other than those close to the bottom. The whale was observed to be actively feeding in some places and merely traversing or searching in others. The cruise track gives an indication of how the whale responded to the prey distribution. There were strong contrasts in backscattering intensity along the entire survey (Fig. 11) and for the separate segments of that survey (indicated in Fig. 11) that were used in the spectral analysis of that data. The spectral density and autocovariance for those segments (Fig. 12) showed that concentrations of patches with dimensions of 0.25–0.5 km (frequencies of 4–2 cycles km^{-1}, respectively) were relatively more common in segment B–B′ than in either of the other two segments. Segment A–A′ possessed some of these components but less than B–B′. Segment C–C′ had a relatively flat spectrum and lower overall abundances (see Fig. 11). In each of these segments, the behavior of the whale (as shown by the cruise track) was different (i.e. turning or proceeding straight ahead).

The data set detailed in Table 2 was examined, by cluster analysis, to determine which

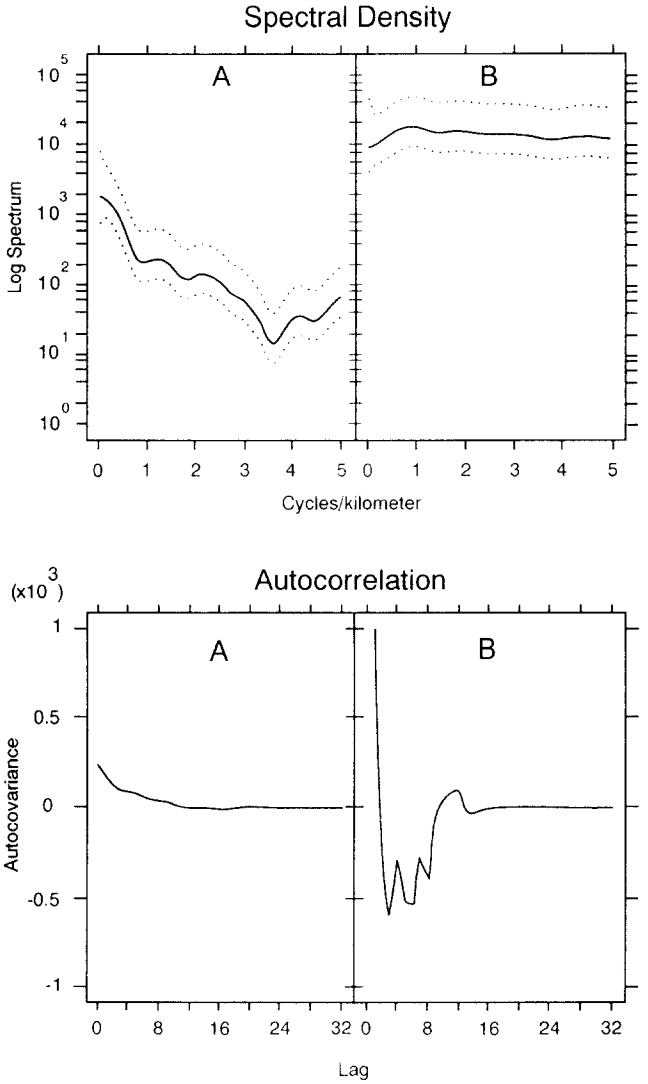

Fig. 8. Spectral density (as log of the spectrum, units of tons^2 km^{-4}/cycles km^{-1} and autocorrelation (units of tons^2 km^{-4}) plots of data from the small scale survey conducted 2 June 1989 in the vicinity of a salinity front. Autocovariance has been divided by 10^3. The dotted lines are 95% confidence limits.

environmental or observed biological parameters were most strongly associated with whale and non-whale areas. The cluster analysis using peak copepod abundance from the nets (CPK) and acoustic estimate of peak abundance (ACOUS), shown in Table 5, idicated that a separation of whale and non-whale sites could be made. A *K*-means procedure determined that the resulting clusters were highly significant ($P = 0.006$ for CPK and $P = 0.0$ for ACOUS).

Cluster analysis was also used to test for changes in whale diving depth by year (Table 6). Selected samples of whale site data were used to compare data from 1988, when the whales

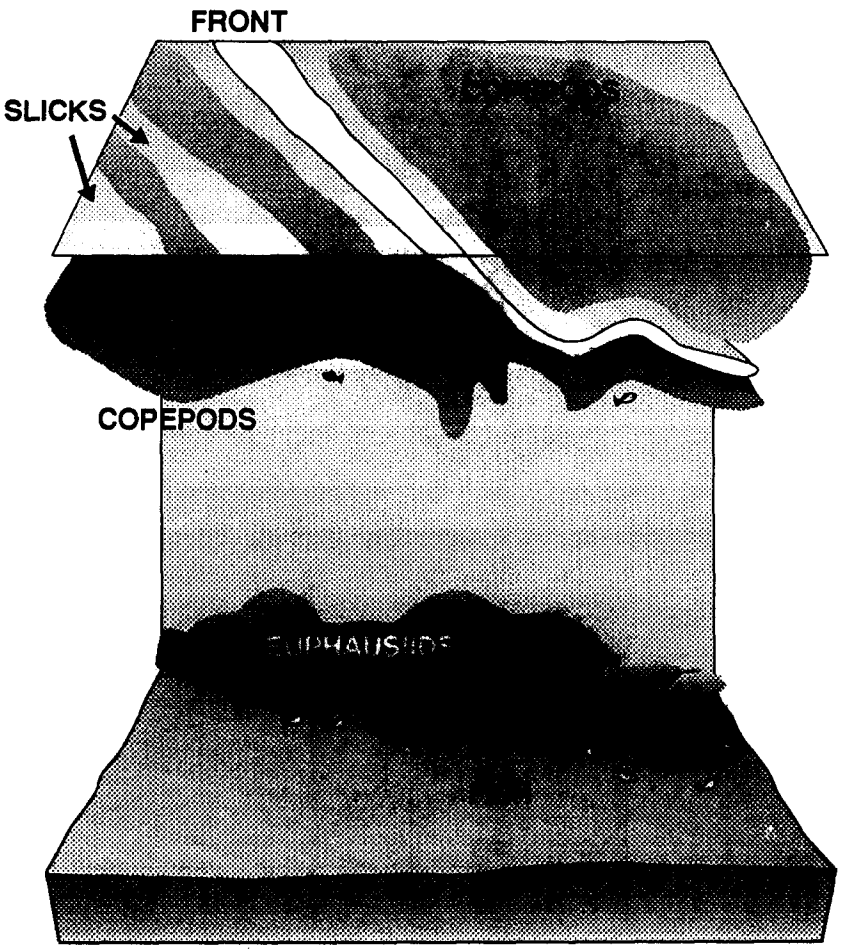

Fig. 9. Schematic diagram of a frontal zone area showing the major features present.

exhibited deeper dives especially during the day, with data from 1989, when the whales exhibited shallower dives (WINN *et al.*, 1995). The observations included day and night samples from both years. The results (Table 6) showed that peak copepod abundance (CPZ) was indeed deeper in 1988 than in 1989 ($P = 0.037$). Acoustic estimates of the depth of peak copepod abundance (AZ) did not show this trend; the acoustic data actually suggest that the peak copepod abundances were shallower in 1988, though not significantly so ($P = 0.351$), partly due to the high variability, shown by the standard deviation in Table 6, of the 1989 AZ data. The observations used were carefully matched with the same ratio of day-to-night (1:1) and maximum depth range in both years and all tests were done on pairs of day–night observations, but because the acoustic data underestimated the abundance of copepods deeper than 50 m, the trend shown by that data was biased toward shallower concentrations. It would have been possible to correct for this deficiency by increasing the signal gain on the acoustic system; unfortunately this was not recognized in time to compensate for it. Based on the net data alone, the conclusion was that the peak copepod depth was deeper in 1988 than in 1989. This was due to the fact that in 1988, there

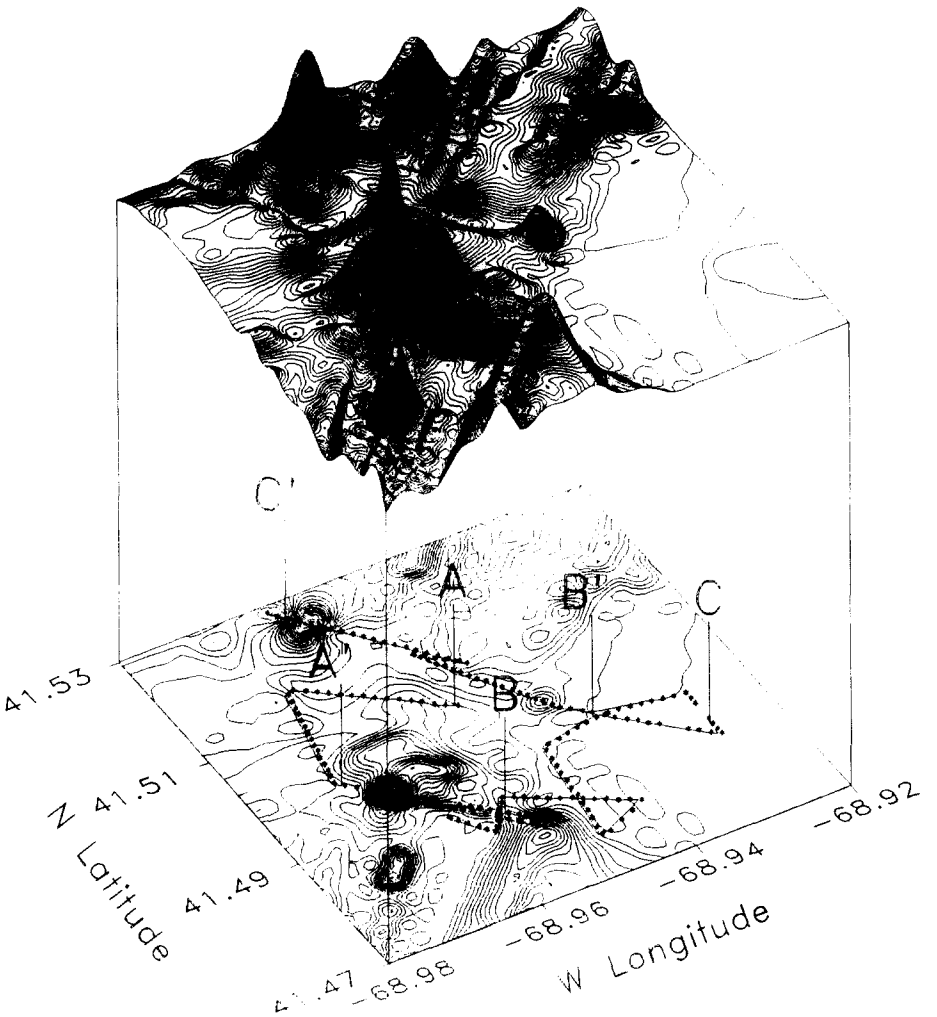

Fig. 10. Distribution of copepods and tagged whale track showing the relation of a tagged right whale to the copepod distribution in the upper 50 m. The line segments shown in the lower plot (A–A', B–B', and C–C') correspond to the segments of data used for analyzing spectral density. Peak abundance for each segment is given in Table 2; the plot of spectral density is Fig. 12. Some features (especially those distant from the cruise track) are extrapolations from trends in the data.

was a strong diel vertical migration in most areas by the copepods, while in 1989, the copepods remained near the surface day and night (WISHNER *et al.*, 1995).

Variables found significant from the initial cluster analyses were used in a step-wise discriminant function analysis (Table 7) to establish a quantitative measure for distinguishing (or otherwise characterizing) whale sites from their counterpart non-whale sites. This analysis determined that, of all the characterizing variables examined as discriminators between whale and non-whale sites, hydroacoustic estimates were the strongest separating variable, then peak copepod abundances, and lastly euphausiid abundances (copepod and euphausiid abundances were from net samples, and all data were from the upper 50 m).

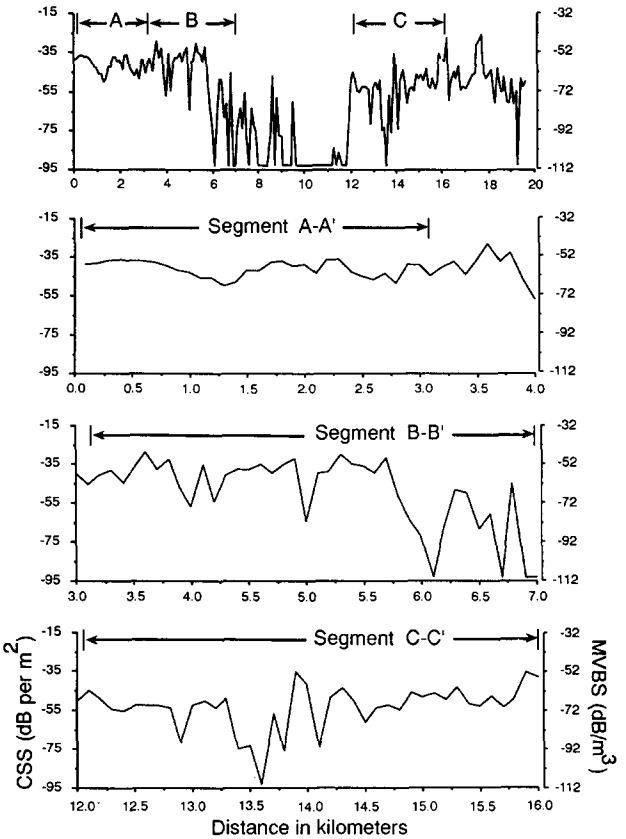

Fig. 11. Target strength free backscatter as column scattering strength (CSS) and mean volume backscattering strength (MVBS) for the entire survey and the line segments shown in Fig. 10. Distance from the start of the survey is given in km.

Data from other SCOPEX areas (i.e. data from "Test" section of Tables 2 and 3) were not used in the determination of the discriminant function; instead this set of observations was used after the discriminant function had been established, as a test of the rigor of the function's ability to identify such areas. In every case examined using these test values, the discriminant function identified the observation as originating from its proper classifying site. This indicates the ability of the discriminant function to properly identify observations other than those used to establish the relationship (i.e. its rigor).

The resulting discriminant functions from Tables 7–9 (constructed to maximize the difference between the selected groupings) are given by

Acoustic estimate only:

$$\text{Non-whale site index} = 0.03977 \times \text{ACOUS} - 0.73544$$
$$\text{Whale site index} = 0.35071 \times \text{ACOUS} - 3.98103.$$

Acoustic estimate plus net estimate:

$$\text{Non-whale site index} = 0.00026 \times \text{CPK} + 0.02978 \times \text{ACOUS} - 1.04893$$
$$\text{Whale site index} = 0.00057 \times \text{CPK} + 0.32892 \times \text{ACOUS} - 5.47193.$$

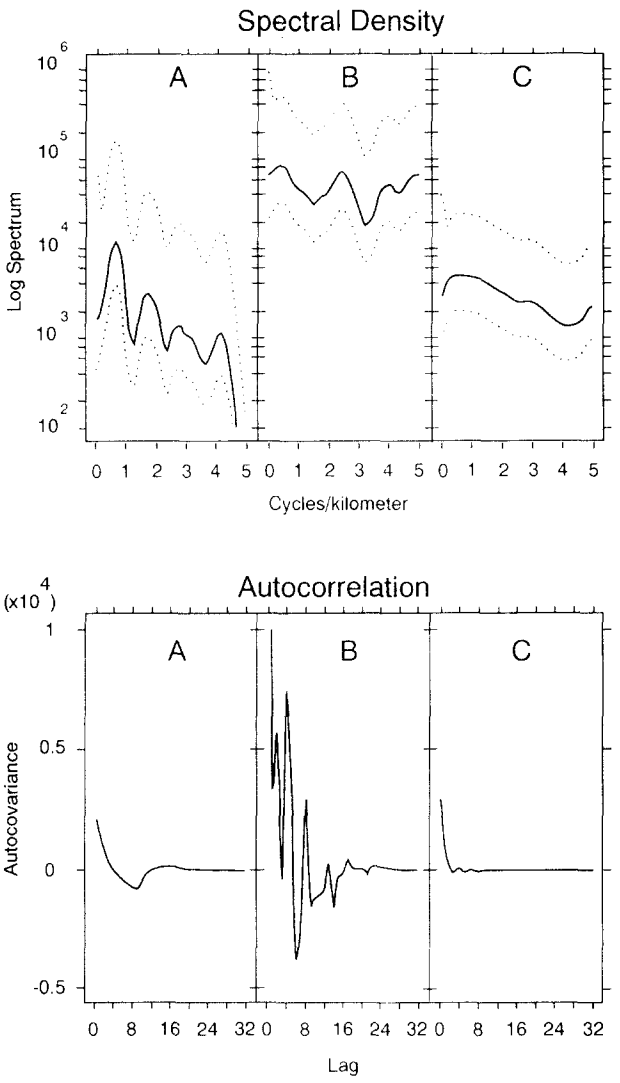

Fig. 12. Spectral density (as log of the spectrum, units of tons^2 km^{-4} cycles km^{-1}) and autocorrelation (units of tons^2 km^{-4}) plots for whale track data by segment. Note the changes in spectral density and their relation to changes in the right whale's track shown in Fig. 9. Autocovariance has been divided by 10^4. The dotted lines are 95% confidence limits.

Net estimate alone:

$$\text{Non-whale site index} = 0.00027 \times \text{CPK} - 1.02542$$
$$\text{Whale site index} = 0.00065 \times \text{CPK} - 2.60434.$$

To classify a new observation, the value of ACOUS (as g m^{-3}, note unit change from values shown in Table 2), CPK (as mg m^{-3}, units are the same as shown in Table 2), or both is used to calculate a value for both the whale and non-whale index. The classification to which the observation belongs is that which produces the larger of the two index values.

Table 5. Dendrogram of clusters formed using copepod density (CPK) and acoustic biomass (ACOUS). Data used were from Table 2. Distances computed using standardized data (z-transform) single linkage method

Case No.	1	2	1	3	4	7	8	2	1 0	9	1 3	1 4	6	5
L	N	N	N	N	N	N	N	N	W	W	W	W	W	W
A	W	W	W	W	W	W	W	W						
B	M	M	M	M	M	M	M	M	M	M	M	M	M	M
E	7	9	9	7	7	9	9	7	9	9	9	9	7	7
L	0	3	2	1	1	0	0	0	1	1	3	3	1	1
	6	2	7	3	4	2	3	7	5	2	5	4	7	5

Distance

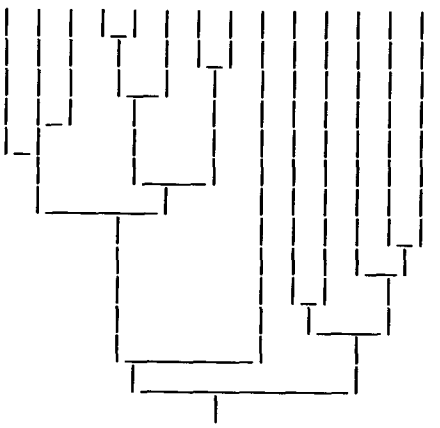

Cluster 1 of 2 contains 5 cases Average distance 1.200
Cluster 2 of 2 contains 9 cases Average distance 0.563

Cluster means

	Size	COK	ACOUS
1	5	7006.6	21.9880
2	9	2250.3	2.1747

Cluster standard deviations

1	3942.88	8.9830
2	1417.46	0.7427
F-Ratio	11.15	46.279
P-Value	0.006	0.000
D.F.	1, 12	1, 12

D.F. = degrees of freedom.

For further discussion of the use of discriminant functions, see LACHENBRUCH and MICKEY (1968). When the Mahalanobis *D*-square is small, the observation is near the mean for the group. Larger values for Mahalanobis *D*-square may indicate either incorrect classification or possible errors. The posterior probability should be close to 1.0 for a correctly classified observation; lower values indicate a lesser fit to the group.

Table 6. Dendrogram of clusters formed using copepod depth (CPZ) and acoustic depth of peak (AZ). Data used were from Table 2. Distances computed using standardized data (z-transform) single linkage method

Case No.	1	3	4	2	6	7	11	10	9	8	5
L	D	D	D	D	S	S	S	S	S	S	S
A	M	M	M	M	M	M	M	M	M	M	M
B	7	7	7	7	9	9	9	9	9	9	9
E	1	0	1	1	1	3	3	2	1	3	1
L	5	8	1	7	5	5	7	2	9	4	2

Distance

0.378
0.378
0.421
0.660
0.785
0.837
1.240
1.411
1.525
2.006

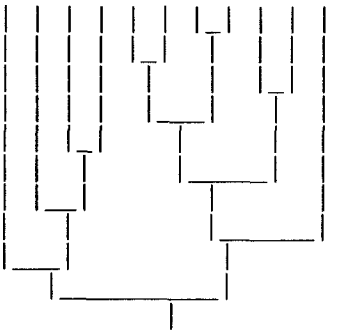

Cluster 1 of 2 contains 7 cases Average distance 0.9765
Cluster 2 of 2 contains 9 cases Average distance 1.1427

Cluster means

	Size	COK	ACOUS
1	7	13.286	16.4286
2	4	42.750	12.0000

Cluster standard deviations

1	6.4476	8.5021
2	32.0663	3.1623
F-Ratio	5.965	0.969
P-Value	0.037	0.351
D.F.	1, 9	1, 9

D.F. = degrees of freedom.

The discriminant function, using acoustic estimates only (Table 7), identified observations collected during a tagged whale tracking experiment (observations labeled SEGA–SEGC in Table 2) as belonging to the whale site group. These three observations were included to test the discriminant function on data taken from locations where we were able to directly observe the presence and behavior of a right whale as well as the populations of its prey. These analyses also showed that when hydroacoustic estimates were included in the stepwise selection, they dominated the discriminant function; net catch estimates of copepod and euphausiid abundance were either not significant or of

Table 7. Discriminant function analysis of biomass parameters using data classified as whale or non-whale to develop the discriminant function and then testing it on additional observations. The variables used were CPK, EUP, CP50, EU50 *and* ACOUS. *Variable* ACOUS *was used alone for the discriminant function. The groups* UN *and* UW *were the test data classified as non-whale* (UN) *and whale* (UW) *observations. The discriminant function was developed using the whale* (W) *and non-whale* (NW) *observations and then tested on the* UN *and* UW *observations*

Variable entered		ACOUS				
Variable	F TO REMOVE			*	Variable	F TO ENTER
DF = 1	12			*	DF = 1	11
ACOUS	17.72			*	CPK	1.11
				*	EUP	1.49
				*	CP50	0.89
				*	EU50	1.50

Classification functions

Group = NW		W
Variable		
ACOUS	0.03977	0.35071
Constant	−0.73544	−3.98103

Jackknifed classification

Group	Percentage correctly	Number of cases classified into group	
		NW	W
NW	100.0	8	0
W	83.3	1	5
UN	100.0	2	0
UW	100.0	0	8
Total	95.8	11	13

	Incorrect classifications		Mahalanobis D-square from, and posterior probability for, group
Group W		NW	W
Case			
10 M915	NW	0.0 0.921	4.9 0.079

much less significance (see "F TO ENTER" section of Tables 7 and 8). When only net catch estimators were used (see Table 9 where ACOUS was excluded), copepod abundance dominated. Overall, acoustic estimates were 95.8% correct in separating whale site from non-whale site data, and net estimates alone (Table 9) were 80.9% successful. This clearly shows that net estimates of copepod abundance and acoustic estimates of copepod abundance can be used to discriminate between whale sites and non-whale sites.

DISCUSSION

The zooplankton samples from net tows provided additional information on other biological attributes of whale areas. These locations were characterized by higher abundances and proportions of the older larger *Calanus* lifestages compared to the overall region, but not necessarily higher total copepod biomasses or abundances, and it has been

Table 8. *Discriminant function analysis of biomass parameters using data classified as whale or non-whale to develop the discriminant function and then testing it on additional observations. The variables used were* CPK, EUP, CP50, EU50 *and* ACOUS. *The variables* CPK *and* ACOUS *were used together for the discriminant function. Observations* SEGA–SEGC *were excluded because they had no matching copepod data. The groups* UN *and* UW *were the test data classified as non-whale* (UN) *and whale* (UW) *observations. The discriminant function was developed using the whale* (W) *and non-whale* (NW) *observations and then tested on the* UN *and* UW *observations*

Variable entered		CPK, ACOUS				
Variable	F TO REMOVE			*	Variable	F TO ENTER
DF = 1	11			*	DF = 1	10
CPK	1. 11			*	EUP	0.66
ACOUS	10.90			*	CP50	0.25
				*	EU50	0.67

Classification functions

Group = NW		W
Variable		
CPK	0.00026	0.00057
ACOUS	0.02978	0.32892
Constant	−1.04893	−5.47193

Jackknifed classification

Group	Percentage correctly	Number of cases classified into group	
		NW	W
NW	100.0	8	0
W	83.3	1	5
UN	100.0	2	0
UW	100.0	0	5
Total	95.2	11	10

	Incorrect classifications		Mahalanobis *D*-square from, and posterior probability for, group
Group W		NW	W
Case			
10 M915	NW	0.4 0.971	7.4 0.029

hypothesized that the whales are seeking out aggregations of older copepods rather than simply the densest aggregations (WISHNER *et al.*, 1995). Older larger lifestages should be stronger acoustic targets than younger smaller lifestages, and this may help explain why the acoustic signal dominated the discriminant function differentiating whale and non-whale areas.

The results shown in Table. 4 indicate that the acoustic estimates of biomass are frequently larger than the net sample measurements. This is especially apparent when comparing net catches of micronekton (total biomass minus copepod biomass) with the acoustic estimates of their abundance. Comparing peak biomasses at the same depth (Table 4, column labeled A/MBT, which is the acoustic estimate divided by the net estimate for the same depth as the acoustic estimate), we see that the agreement is not good. The peak estimates at the same depth show four of the 17 cases within a factor of 2

Table 9. Discriminant function analysis of biomass parameters using data classified as whale or non-whale to develop the discriminant function and then testing it on additional observations. The variables used were CPK, EUP, CP50 *and* EU50. *The variable* CPK *was used alone for the discriminant function. Observations* SEGA–SEGC *were excluded because they had no matching copepod data*

Variable entered		CPK				
Variable	F TO REMOVE		*	Variable	F TO ENTER	
DF = 1	12		*	DF = 1	11	
CPK	4.45		*	7 EUP	0.05	
			*	9 CP50	2.68	
			*	10 EU50	0.07	

Classification functions		
Group = NW		W
Variable		
CPK	0.00027	0.00065
Constant	−1.02542	−2.60434

Jackknifed classification

Group	Percentage correctly	Number of cases classified into group	
		NW	W
NW	87.5	7	1
W	66.7	2	4
UN	100.0	2	0
UW	60.0	2	3
Total	80.9	13	8

	Incorrect classifications		Mahalanobis *D*-square from, and posterior probability for, group
Group NW		NW	W
12 M932	W	0.5 0.468	0.2 0.532
Group W		W	UW
5 M715	NW	0.0 0.657	1.3 0.343
10 M915	NW	0.4 0.801	3.2 0.199
Group UW		NW	W
15 M708	NW	0.2 0.753	2.4 0.247
19 M919	NW	0.0 0.652	1.3 0.348

and nine of the 17 within a factor of 4 of each other. In two cases (M708 and M715) the acoustic estimate is much higher than the net estimate. In both of these cases, a patch of targets (from appearances, each was assumed to be copepods) were observed acoustically at a time when the MOCNESS was at a different depth, i.e. the difference is attributable to the small-scale patchiness problem and the difference between a continuous sampler (the acoustic system) and a discrete sampler (the net). In three of the five cases where the ratio of acoustic estimate to net estimate was greater than 4, there is indication in the net samples of the presence of euphausiids (see Table 2 for matching cases); thus the difference may be the result of including some non-copepod targets in the acoustic estimates. For eight of the 20 comparisons, the ratio of acoustic estimate to net estimate in the upper 50 m was less than or equal to 1. It would seem that both sampling devices

provide a similar view of the distribution of copepods, though somewhat different in specific detail, because of the inherent nature of the sampling accomplished with each device. For example, net estimates of biomass are derived from large volumes of water, but acoustic estimates are from a smaller volume (200 m^3 or more for nets and 60–100 m^3 for acoustic samples).

The estimated range of error associated with target strength is about ±3 dB (between models and measured values for the same size target). This is equivalent to a product/quotient factor of 2 (or 1/2) times the acoustically estimated biomass. Our experience with a large variety of horizontal and vertical net haul replicates indicates that a product/quotient factor of 1 to several times net catch biomasses is commonly encountered between net haul replicates, the larger differences often being associated with the presence of small-scale hydrographic or dynamic features. Many of the cases where the net estimated biomass varies from the acoustic estimate by a product/quotient factor of only 2–3 may not really be substantially different.

Where concentrations of plankton have limited dimensions, net samples will always produce lower estimates of biomass due to sampling (variable) volumes containing lower abundances of organisms. We consider both types of samples to be representative of the populations sampled, with acoustic samples providing a better estimate of the maximum concentration available to predators like the right whale. At the electronic settings used in this study, it is likely that the acoustic estimate of copepod biomass is adequate from 0 to 75 m, but probably underestimates copepods (especially the smaller stages) deeper than 75 m. Net catch data are undoubtedly better estimates of abundance for deeper, smaller stages than the acoustic data for these same depths. Future studies of this kind should employ high source levels from the sounder system by using narrower beam transducers, higher gain on the receiver (which would increase noise level as well, but there should still be sufficient signal), or by towing the transducer array deeper to maintain the range at less than 75 m. Deep towed transducers could be deployed in a bi-directional mode looking upward and downward to provide full water column coverage. The bi-directional approach would, however, create a narrow band above and below the transducer of 3–5 m which would be in the near field of the transducers and hence would provide no means of estimating scattering in that depth band.

It is clear from Figs 6–8 that the spatial scales of patches of copepods are distinctly different between areas north and south of the front within the small scale survey area from 1989. In Fig. 8, the 95% confidence interval (dotted lines on the spectral density plots) can be used to determine where statistically significant differences are present in spectral density. In general, patterns of spectral density observed for zooplankton distributions are often flat over most spatial scales less than 1 km (frequencies greater than 1 cycle km^{-1}), unlike a slope of −5/3 in spectral density often exhibited by phytoplankton (cf. PLATT and DENMAN, 1975; WEBER *et al.*, 1986), and somewhat like section A–A′ for frequencies less than 1 cycle km^{-1} where the spectral density plot slopes sharply downward. Peaks or low points in the distribution, and especially a flat spectral density, suggest that aggregating behavior as well as physical forces may be determining the distribution of zooplankton, rather than their being distributed as purely neutral particles (as is more nearly the case for phytoplankton). Strong currents can cause dispersal of zooplankton (especially weaker swimmers like copepods) and result in low points in the spectral density. Local concentrating factors (e.g. physical processes such as convergence zones, concentrations of food, or aggregating behavior) could produce peaks in the spectral density. The strong dichotomy

in distribution of copepods observed in the frontal region of this small scale study may represent examples of both dispersing and concentrating factors dominating to different degrees.

Evidence for right whales modifying their behavior in response to changes in scale factors of copepod patches was examined by spectral analysis of the hydroacoustic data collected when a radio tagged invididual whale was being followed. There clearly are changes in direction (shown by the shape of the cruise track as the ship stayed some distance from the whale) as it progressed through the area. These differences seem well correlated with the locations of concentrations of copepods (Fig. 10), with changes in abundances of copepods (Fig. 11), and with the spectral density of patch size (Fig. 12). The whale behaved differently in an area containing patches of copepods with a scale size of 0.5–0.3 km (segment B–B′) by crossing and re-crossing its path. MAYO and MARX (1990) found similar evidence that right whales modify their behavior in response to the density of the prey field. A patch size similar to that shown in Fig. 10 (0.5–0.3 km) was found in horizontally sequenced MOCNESS tows in the area (WISHNER *et al.*, 1995).

The autocorrelation plot for segment B–B′ shows a high degree of autocorrelation at lags of 2, 4 and 8. This suggests that abundances were similar at 200, 400 and 800 m scales (i.e. the spacing between concentrations of copepods is similar at these scales). The cross and re-cross pattern of behavior was also observed, to a lesser extent, in an area with lower copepod abundance (segment A–A′). In both these areas (A–A′ and B–B′), the whale altered its path as if it were searching for a particular feature or features in the food distribution. When the area contained a scarcity of concentrations with the above dimensions (e.g. segment C–C′) the whale continued on a more steady course. The observations SEGA-SEGC used in the discriminant function analysis above (Table 7) were taken from these same three segments. The prey densities within the aggregations observed in segments A–A′ and B–B′ are within the limits required to provide adequate caloric intake for right whales (KENNEY *et al.*, 1986). A conclusion which could be drawn from these observations is that maximum concentration may not be the only feature of importance to right whales in selecting feeding areas; the distribution of aggregations (by size or depth of concentration) may also be a factor in a whale's preference for a particular site in which to feed.

CONCLUSIONS

Hydroacoustic estimates of backscatter from the SCOPEX project are strongly related to the distribution and abundance of several types of zooplankton. The relation of the distribution and abundance of zooplankton to environmental features (fronts, surface slicks, etc.) can be examined in detail by hydroacoustic methods. Cluster analysis on selected samples of the hydroacoustic data showed that acoustically estimated biomass and net samples could be strong indicators of areas of biological activity. The influence of physical features of the environment on biological distribution can be demonstrated using spectral density analyses. Results of an FFT analysis for spectral composition and autocovariance using hydroacoustic observations showed that there were strong contrasts in the spectral density at a frontal feature (predominantly a salinity front in the case examined), as opposed to away from the front, and significant differences between areas where a whale spends more time (presumably or observably feeding) and where it moves more rapidly (presumably searching for food). The behavior of whales, in particular the

right whale, can be shown to be related to the spatial scales and abundance of their prey using hydroacoustic estimates of target distribution and abundance. The application of this methodology to the study of zooplankton demography and predator–prey interaction provides a means of greatly increasing the spatial and temporal resolution of observations and overcomes some inherent limitations of other forms of directed sampling.

Acknowledgements—We thank K. Sherman of NMFS (for providing us with sampling time on the R.V. *Delaware II*), J. Green, J. Sibunka, the URI marine technical group, and the captains, crews and other SCOPEX investigators on the Delaware and Endeavor who generously assisted us with cruise preparations and sampling at sea. We thank Pat Morrison for her assistance in the sampling and analysis of acoustic data, C. Ashjian and R. Campbell for their help, and many students for sorting the plankton. The 1986 pilot program was supported by ONR contract NR 4221013–01 to M. Macaulay and B. Frost, N00014-86-K-0373 to K. Wishner, A. Durbin and E. Durbin, and aerial surveys supported by MMS order no. 12504 to H. Winn and R. Kenney. Support for the hydroacoustics during SCOPEX was provided by NSF grants OCE89-04247 and OCE89-15844. The latter two grants were funded by Minerals Management Service through NSF. The zooplankton net sampling was supported by NSF grants OCE87-11847 and OCE89-15610. The physical oceanography was supported by NSF grants OCE87-13988 and OCE91-01034. Whale studies were supported by NSF grant OCE89-15610.

REFERENCES

AMERICAN NATIONAL STANDARDS INSTITUTE, INC. (1972) *Procedures for calibration of underwater electroacoustic transducers*, American National Standards Institute, Inc., 1430 Broadway NE, New York, 40 pp.

BARRACLOUGH W. E., R. J. LEBRASSEUR and O. D. KENNEDY (1969) Shallow scattering layer in the subarctic Pacific Ocean: Detection by high frequency echo sounder, *Science*, **166**(3905), 611–612.

BMDP (1990) *BMDP PC-90*, BMDP Statistical Software, Inc., Los Angeles, California.

CETACEAN and TURTLE ASSESSMENT PROGRAM (1982) *A characterization of marine mammals and turtles in the Mid- and North Atlantic areas of the U.S. Outer Continental Shelf, Final Report*. Contract #AA551-CT8-48, Bureau of Land Management, U.S. Dept. of Interior. Washington, D.C., 576 pp.

CHEN C., R. C. BEARDSLEY and R. LIMEBURNER (1995). Variability of water properties in late spring in the northern Great South Channel, *Continental Shelf Research*, **15**, 415–431.

CUSHING D. H. (1978) The present state of acoustic survey. *Journal du Conseil International pour l'Exploration de la Mer*, **38**(1), 28–32.

GREENLAW C. F. (1977) Backscattering spectra of preserved zooplankton: *Journal of the Acoustical Society of America*, **62**(1), 44–52.

HAMMING R. W. (1977) *Digital filters*. Prentice Hall, Englewood Cliffs, New Jersey.

JOHANNESSON K. A. and R. B. MITSON (1983) *Fisheries acoustics: a practical manual for aquatic biomass estimation*. FAO Fisheries Technical Paper 240. FIRM/T240, FAO Rome, 249 pp.

JOHNSON R. K. (1977) Sound scattering from a fluid sphere revisited. *Journal of the Acoustical Society of America*, **61**(2), 375–377.

KENNEY R. D., M. A. M. HYMAN, R. E. OWEN, G. P. SCOTT and H. E. WINN (1986) Estimation of prey densities required by western North Atlantic right whales, *Marine Mammal Science*, **2**(1), 1–13.

KENNEY R. D., H. E. WINN and M. C. MACAULAY (1995) Cetaceans in the Great South Channel 1979–1989: right whales (*Eubalaena glacialis*). *Continental Shelf Research*, **15**, 385–414.

KRISTENSEN A. (1983) *Acoustic classification of zooplankton*. ELAB Report Series STF44 A83187, 112 pp.

LACHENBRUCH, P. and R. M. MICKEY (1968) Estimation of error rates in discriminant analyses. *Technometrics*, **10**, 1–11.

LIMEBURNER R. and R. C. BEARDSLEY (1989) *CT observations in the Great South Channel during the South Channel Ocean Productivity EXperiment, SCOPEX, May–June* 1989. WHOI Technical Report. 89–51, 252 pp.

LOEB V. J., A. F. AMOS, M. C. MACAULAY, J. H. WORMUTH (1993) Antarctic krill stock distribution and composition in the Elephant Island and King George Island areas, January–February, 1988. *Polar Biology*, **13**, 171–181.

MACAULAY M. C. (1978) Acoustic assessment of zooplankton. Ph.D. Dissertation. University of Washington, Seattle, Washington, (unpublished), 139 pp.

MACAULAY M. C., T. S. ENGLISH and O. A. MATHISEN (1984) Acoustic characterization of antarctic krill (*Euphausia superba*) swarms from Elephant Island and Bransfield Strait. Special Issue **4** of *Journal of Crustacean Biology*, pp. 16–44.

MACLENNAN D. N. and E. J. SIMMONDS (1992) *Fisheries acoustics*. Fish and Fisheries Series 5, Chapman and Hall, London, United Kingdom, 325 pp.

MATHISEN O. A. (1980) *Methods for the estimation of krill abundance in the Antarctic*. National Technical Information Service, Department of Commerce PB80-175151, 26 pp.

MATHISEN O. A. and M. C. MACAULAY (1983) The morphological features of a superswarm of Krill, *Euphausia superba*. *Memoirs of National Institute of Polar Research. Special Issue* **27**, National Institute of Polar Research, Tokyo, pp. 153–164.

MACAULAY M. C. and O. A. MATHISEN (1991) AMLR PROGRAM: Hydroacoustic observations of krill distribution and biomass near Elephant Island, Summer 1991. *Antarctic Journal of the United States*, **26**(5), 203–204.

MAYO C. A. and M. K. MARX (1990) Surface foraging behavior of the North Atlantic right whale, *Eubalaena glacialis*, and associated zooplankton characteristics. *Canadian Journal of Zoology*, **68**, 2214–2220.

MIDTTUN L. and O. NAKKEN (1968) Counting of fish with an echo-integrator. *International Council for Exploration of the Sea Cooperative Research Report Series B*, **17**(9).

PLATT T. and K. L. DENMAN (1975) Spectral analysis in ecology. *Annual Review of Ecology and Systematics*, **6**, 189–210.

RICHTER K. E. (1985) Acoustic scattering at 1.2 MHz from individual zooplankters and copepod populations. *Deep-Sea Research*, **32**(2), 149–161.

SWINGLER D. N. and I. HAMPTON (1981) Investigation and comparison of current theories for the echo-integrator technique of estimating fish abundance, and their verification by experiment. In: *Meeting on hydroacoustic methods for the estimation of marine fish populations*, 23–29 *June* 1979. *Vol II*, J. B. SUOMALA, editor, Charles Stark Draper Lab. Inc., Cambridge, Massachusetts, 964 pp.

THORNE R. E. (1971) Investigations into the relationships between integrated echo voltage and fish density. *Journal of the Fisheries Research Board of Canada*, **28**, 1269–1273.

WEBER L. H., S. Z. EL-SAYED and I. HAMPTON (1986) The variance spectra of phytoplankton, krill, and water temperature in the Antarctic Ocean south of Africa. **33**, 1327–1343.

WIEBE P. H., C. H. GREENE, T. K. STANTON and J. BURCZNSKI (1990) Sound scattering by live zooplankton and micronekton: Empirical studies with a dual beam acoustic system. *Journal of the Acoustical Society of America*, **88**, 2346–2360.

WINN H. E., J. D. GOODYEAR, R. D. KENNEY and R. O. PETRICIG (1995) Dive patterns of tagged right whales in the Great South Channel. *Continental Shelf Research*, **15**, 593–611.

WISHNER K., E. DURBIN, A. DURBIN, M. MACAULAY, H. WINN and R. KENNEY (1988) Copepod patches and right whales in the Great South Channel off New England. *Bulletin of Marine Science*, **43**, 825–844.

WISHNER K. F., J. R. SCHOENHERR, R. BEARDSLEY and C. CHEN (1995) Abundance, distribution, and population structure of the copepod *Calanus finmarchicus* in a springtime right whale feeding area in the southwestern Gulf of Maine. *Continental Shelf Research*, **15**, 475–507.